Genotoxicity in the absence of inflammation after tungsten inhalation in mice

Sørli, Jorid B.; Jensen, Alexander C.Ø.; Mortensen, Alicja; Szarek, Józef; Gutierrez, Claudia A.T.; Hafez, Iosif; Biskos, George; Hougaard, Karin S.; Vogel, Ulla; More Authors

DOI
10.1016/j.etap.2023.104074

Publication date
2023

Document Version
Final published version

Published in
Environmental Toxicology and Pharmacology

Environmental Toxicology and Pharmacology 98 (2023) 104074

Contents lists available at ScienceDirect

Environmental Toxicology and Pharmacology

journal homepage: www.elsevier.com/locate/etap

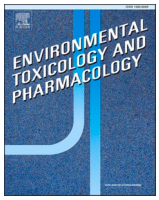

Genotoxicity in the absence of inflammation after tungsten inhalation in mice

Jorid B. Sørli [a,*], Alexander C.Ø. Jensen [a], Alicja Mortensen [a], Józef Szarek [b], Eleni Chatzigianelli [a], Claudia A.T. Gutierrez [a,c], Nicklas R. Jacobsen [a], Sarah S. Poulsen [a], Iosif Hafez [d], Charis Loizides [d], George Biskos [d,e], Karin S. Hougaard [a,f], Ulla Vogel [a,g], Niels Hadrup [a,h,**]

[a] National Research Centre for the Working Environment (NFA), 105 Lersø Parkallé, Copenhagen Ø, Denmark
[b] Department of Pathophysiology, Forensic Veterinary Medicine and Administration, University of Warmia and Mazury in Olsztyn, Olsztyn, Oczapowskiego 13, 10-719 Olsztyn, Poland
[c] Department of Public Health, University of Copenhagen, Copenhagen, Denmark
[d] Climate and Atmosphere Research Centre, The Cyprus Institute, 20 Konstantinou Kavafi Street, 2121, Aglantzia Nicosia, Cyprus
[e] Faculty of Civil Engineering and Geosciences, Delft University of Technology, Gebouw 23 Stevinweg 1, 2628 CN Delft, the Netherlands
[f] Department of Public Health, University of Copenhagen, Øster Farimagsgade 5, 1353 Copenhagen K, Denmark
[g] DTU Food, Technical University of Denmark, Kemitorvet Bygning 202, 2800 Kongens Lyngby, Denmark
[h] Research group for Risk-benefit, National Food Institute, Technical University of Denmark, Kemitorvet Bygning 202, 2800 Kongens Lyngby, Denmark

ARTICLE INFO

Edited by Dr. M.D. Coleman

Keywords:
Comet assay
Wolfram
Pulmonary
Toxicity
Toxicology

ABSTRACT

Tungsten is used in several applications and human exposure may occur. To assess its pulmonary toxicity, we exposed male mice to nose-only inhalation of tungsten particles at 9, 23 or 132 mg/m^3 (Low, Mid and High exposure) (45 min/day, 5 days/week for 2 weeks). Increased genotoxicity (assessed by comet assay) was seen in bronchoalveolar (BAL) fluid cells at Low and High exposure. We measured acellular ROS production, and cannot exclude that ROS contributed to the observed genotoxicity. We saw no effects on body weight gain, pulmonary inflammation, lactate dehydrogenase or protein in BAL fluid, pathology of liver or kidney, or on sperm counts. In conclusion, tungsten showed non-dose dependent genotoxicity in the absence of inflammation and therefore interpreted to be primary genotoxicity. Based on genotoxicity, a Lowest Observed Adverse Effect Concentration (LOAEC) could be set at 9 mg/m^3. It was not possible to establish a No Adverse Effect Concentration (NOAEC).

1. Introduction

Tungsten is used in a number of applications including in the automotive, medical and mining industries. It has lubricating properties, and was initially taken into use in space, but is now also used in general spray-formulated lubricants (Sørli et al., 2022). It is also a component of industrial hard steel, and may therefore also occur in welding fumes (Graczyk et al., 2016). The knowledge of occupational air concentrations of tungsten seems very limited. One investigation of the Swedish hard metal industry reported powder production to be the work process that resulted in the highest tungsten air concentration (0.11 mg tungsten/m^3) (Klasson et al., 2016). To minimise the risk of adverse health effects from exposure to this metal, it is important to determine the level at which it becomes toxic. Although inhalation of tungsten in pure form can be foreseen e.g. during the manufacture of products in which it is a constituent; inhalation of tungsten in a mixture with other substances seems more likely. In the latter instance, knowledge of its toxicity can be included in mathematical models for assessing the combined toxicity of the whole exposure (Hadrup, 2014; Hadrup et al., 2013; Scholze et al., 2014).

Abbreviations: BAL, bronchoalveolar; ROS, reactive oxygen species.

* Corresponding author.
** Corresponding author at: National Research Centre for the Working Environment (NFA), 105 Lersø Parkallé, Copenhagen Ø, Denmark.
E-mail addresses: jbs@nfa.dk (J.B. Sørli), alexander.co.jensen@gmail.com (A.C.Ø. Jensen), aam@nfa.dk (A. Mortensen), szarek@uwm.edu.pl (J. Szarek), lenachatz11@gmail.com (E. Chatzigianelli), xcag@nfa.dk (C.A.T. Gutierrez), nrj@nfa.dk (N.R. Jacobsen), sspoulsen84@gmail.com (S.S. Poulsen), i.hafez@cyi.ac.cy (I. Hafez), c.loizides@cyi.ac.cy (C. Loizides), g.biskos@cyi.ac.cy (G. Biskos), ksh@nfa.dk (K.S. Hougaard), ubv@nfa.dk (U. Vogel), nih@nfa.dk (N. Hadrup).

https://doi.org/10.1016/j.etap.2023.104074
Received 6 December 2022; Received in revised form 26 January 2023; Accepted 28 January 2023
Available online 29 January 2023

We recently reviewed the pulmonary toxicity of tungsten (Hadrup et al., 2022), but did not identify inhalation studies with the pure metal. Data on other tungsten substances were however available. One study exposed Syrian hamsters to tungsten trioxide (WO_3) nanoparticles by inhalation at levels of 5 or 10 mg/m^3, 4 h/day for 4 or 8 days. At the highest exposure level, the WO_3 nanoparticles induced pulmonary inflammation determined as increased neutrophil numbers in bronchoalveolar (BAL) fluid, as well as elevated lactate dehydrogenase (LDH) and total protein in the same fluid (No Observed Adverse Effect Concentration $(NOAEC)_{BAL\ neutrophils}$: 5 mg WO_3/m^3, = 4 mg W/m^3). Alkaline phosphatase, among other markers, was increased already at 5 mg WO_3/m^3 (Prajapati et al., 2017). Rajendran and co-workers exposed rats to tungsten blue oxide (69% WO_3, 8% $W_{25}O_{73}$, and 23% $W_{20}O_{58}$) at ~63, 257 or 514 mg W/m^3, 6 h/day for 28 days, with post-exposure periods of 8 and 14 days. The lung weight was elevated at all dose levels. Alveolar pigmented and so-called foamy macrophages were observed in all exposed groups but not in controls (Lowest Observed Adverse Effect Concentration ($LOAEC_{Lung\ weight/histopathological\ findings}$: 63 mg W/m^3, the lowest dose level tested) (Rajendran et al., 2012).

One study, using intratracheal instillation in rats, looked at pure tungsten and tungsten in combination with other metals. A dose of 20 mg/kg bw of pure tungsten did not affect neutrophil numbers in BAL fluid, while neutrophils were increased by a combination material of tungsten (92%), nickel (5%), and cobalt (3%) (WNiCo), at 20 mg/kg bw (Roedel et al., 2012). Peão et al. (1993) dosed calcium tungstate ($CaWO_4$) particles (2–10 μm in size) to mice by intratracheal instillation (8 mg W/kg bw), and found increased neutrophils in BAL fluid. Tungsten carbide (WC) has been investigated for pulmonary toxicity in animal studies using intratracheal instillation, mostly with no or limited effects (Huaux et al., 1995; Lardot et al., 1998; Lasfargues et al., 1995, 1992).

Concerning the endpoint of genotoxicity, oral studies with pure tungsten showed increased levels of DNA strand breaks in the comet assay in the bone marrow of mice (Guilbert et al., 2011; Kelly et al., 2013). When WO_3 nano- and micron-sized particles were given to rats by gavage, only the nanoparticles increased the number of micronuclei in bone marrow cells, and the levels of DNA-strand breaks in the comet assay (blood lymphocytes and liver) (Chinde et al., 2017). Tungsten in combination with cobalt was genotoxic in terms of increased micronuclei numbers in pneumocytes after inhalation (oropharyngeal aspiration) (Sironval et al., 2020). There is also evidence of in vitro genotoxicity of tungsten as seen in numerous studies summarised in (Hadrup et al., 2022).

Overall, the knowledge of pulmonary toxicity of pure tungsten is limited. Therefore, we set out to determine the airway exposure levels at which tungsten exhibits inhalation toxicity. We aimed to set dose descriptors (NOAECs/LOAECs). For this, we exposed mice to tungsten by inhalation of 9, 23 or 132 mg/m^3 (Low, Mid and High exposure) (45 min/day, 5 days/week for 2 weeks). In absence of knowledge of the inhalation of pure tungsten, we set these levels based on toxicity data for other tungsten substances. We measured toxicologically relevant endpoints, including body weight gain, pulmonary inflammation, pathology of the liver and kidney, genotoxicity, plasma testosterone, and sperm counts.

2. Material and methods

2.1. Test material

Tungsten Powder (CAS number: 7440–33–7) with a grain size of < 1 μm and a purity of 99.95% (metal basis) according to the manufacturer, was obtained from Alfa Aesar (Kandel, Germany, Prod. No. 44210).

The specific surface area of the test powders was analysed by nitrogen absorption Brunauer–Emmett–Teller (BET) theory analysis (3 P sync 110). During these measurements the samples were dried at 200 °C under vacuum for 2 h, weighed and analyzed with the static volumetric method, using N_2 as adsorbate, and a sample weight of 2.5708 g.

The tungsten powder was aerosolised using a venturi-type rotating disc microfeeder (Fraunhofer Institute für Toxicologie und Aerosolforschung, Hannover, Germany) with a pre-pressure of 5 bar. The aerosolised tungsten powder was led through an aerosol mixing and sedimentation glass tube to the exposure chamber. The total volume-flow was 20 L/min. Samples of the total suspended tungsten powder mass were collected and the aerosol mass concentrations were determined gravimetrically by filter sampling on Millipore Fluoropore filters (⌀ 2.5 cm; pore size 0.45 μm) using an Apex2™ personal sampling pump (Casella, Buffalo, USA) at a flow rate of 2 L/min. During the experiment, chamber air was sampled on pre-weighed filters for the first 45 min for filtered air control and Low exposure, 20 min for Mid exposure and 5 min for High exposure. Filters were weighed on a Sartorius Microscale (Type M3P 000 V001). The filters were acclimatised at 50% relative humidity at 20 °C for at least 24 h before the post-sampling weighing (limit of detection: 0.005 mg/filter). The resulting calculated mass concentrations in the sampled air were 9 ± 6, 23 ± 7 and 132 ± 56 mg/m^3 for Low, Mid and High exposure, respectively. The particle number concentration and aerodynamic particle size distributions of the aerosolisation method were determined using an Electrical Low Pressure Impactor (ELPI+, Dekati Ltd., Tampere, Finland), which measured in 14 size channels between 6 nm and 10 μm at 1 s time resolution.

The estimated alveolar deposition was calculated based on an estimated pulmonary deposited mass rate using the Multiple-Path Particle Dosimetry Model (MPPD) (version 3.04, ARA, Huntsville, AL United States), using exposure levels (9, 23 and 132 mg/m^3), exposure time (45 min) and 10 days of exposure. MMAD and GSD were determined on basis of the mode of the aerosol (Supplemental Fig. S1). Input parameters in the MPPD model are detailed in the Supplemental Materials.

2.2. Animal procedures

The experiments were carried out in accordance with the Danish Animal Experimentation Act (LBK nr 474 of 15/05/2014 and BEK nr 12 of 07/01/2016) and the EU-directive 2010/63/EU on the protection of animals used for scientific purposes. Permission for the study was obtained from the Animal Experimentation Inspectorate, Ministry of Food, Agriculture and Fisheries of Denmark (License No. 2019–15–0201–00114) and the local animal ethics committee. In total, 33 male BALBC/J mice, 8 weeks old (1 for the pilot study and 32 for the main study), were purchased from Janvier Labs (France). The mice were delivered from Janvier in two batches to ensure that the mice were at the same age at exposure onset. Upon arrival, the animals were randomly distributed into cages with either controls or one of the three exposure levels of tungsten (n = 2 animals per cage and n = 8 per group, n = 32 in total). The animals were given ad libitum access to tap water and feed (Altromin no. 1324, Brogaarden, Denmark). Housing was in 1290D eurostandard Type 3 polypropylene cages with Enviro-Dri bedding (Brogaarden, Gentofte, Denmark), and wood blocks served as enrichment (Brogaarden, Gentofte, Denmark). The mice were kept under a 12-h light/12-h dark cycle (light on from 6 a.m.), with a room temperature of 20 ± 2 °C and humidity at 50 ± 20%. The animals had 1–2 weeks of acclimatisation before the experiment was started. For the experiment, the mice were exposed nose-only by placing them in glass rockets that were subsequently inserted into the inhalation chamber.

We identified no toxicological inhalation studies on pure tungsten in the peer-reviewed literature. Thus, we set the exposure levels based on the aforementioned literature on WO_3 (Prajapati et al., 2017; Rajendran et al., 2012). A range of approximately 10–100 mg/m^3 was chosen in to be able to observe a toxicological response in the animals. Yet we acknowledge that one of the few studies with occupational exposure levels reported a concentration of up to 0.1 mg tungsten/m^3 during powder handling (Klasson et al., 2016) – considerably lower than our lowest exposure level. On the other hand, the current Danish occupational exposure limit for tungsten particles is 5 mg/m^3 for an 8-hour working day (Arbejdstilsynet, 2023), corresponding to 53 mg/m^3

during a 45 min exposure. A pilot study was undertaken to set the highest exposure level, using one mouse. The exposure duration was 45 min per day for 3 days and the animal was monitored for an additional 3 days. The tungsten mass concentration during the pilot study was 132 mg/m^3 based on filter measurements, as described above.

In the main study, the tungsten concentrations in the animal's breathing zone were set to 0, 9, 23 and 132 mg/m^3, based on the pilot study. Animals were in total exposed 10 times for 45 min on all weekdays, over two weeks. For half of the controls and all Low exposure mice, exposure began on a Monday (and the mice were killed on a Friday), the Mid exposure began on the ensuing Friday (i.e. 4 days later, with mice killed on a Thursday). For the remaining half of the controls and the High exposure, exposure began on the Monday 3 weeks after the first exposures were initiated (with animals killed on a Friday). The latter animals were purchased 3 weeks after the first animals but were of the same age at arrival (8 weeks old) and at exposure onset. The staggered start had the advantage that potential toxicity at the Low and Mid exposure could be detected before starting up the High exposure. All animals were killed immediately after the last exposure so the recovery time was the same for all the animals. Also, we emphasise that all samples were frozen down or fixed for BAL cell counting on the day the animals were killed, and later measured as one batch. We have previously demonstrated that the samples for the comet assay can be frozen until the day of analysis without the loss of signal (P Jackson et al., 2013a, 2013b). The disadvantage of the setup was that the Mid exposure group had two weekends during their treatment period, as compared to only one weekend for the other groups and were 4 days older than the other animals. The total time the mice spent in the chamber was 60 min per day, including set-up and exposure. Controls were placed in the chamber and were exposed to filtered air under the same airflow conditions and noise levels as those experienced by the treated animals.

Immediately after the last exposure, the animals were anesthetised by subcutaneous injection of a combination of Zoletil 100 (zolazepam 250 mg/mL plus tiletamine 250 mg/mL), Xysol (xylazine 20 mg/mL) and Fentadon (fentanyl 50 μg/mL) in sterile saline, at a volume of 0.1 mL/10 g bw. The animals were killed by exsanguination by withdrawal of heart blood. Next, the mice were opened and the thorax monitored for macroscopic abnormalities such as discolorations, ascites or bleeding. Lung, liver, kidneys, and testes were excised and processed for subsequent analyses.

2.3. BAL fluid cellularity and biochemistry

BAL fluid cellularity was determined as previously described (Kyjovska et al., 2015). BAL fluid protein was determined with a Pierce BCA Protein Assay Kit from Thermo Scientific (Product number 23227) as described in the manufacturer's protocol. Lactate dehydrogenase (LDH) was measured in BAL fluid with an ELISA kit from Abcam (Product number: 02526).

2.4. Genotoxicity measurements

DNA strand break levels were measured in BAL cells, lung and liver tissue as tail per cent DNA, evaluated by the comet assay with the IMSTAR PathFinder system, as described in (P Jackson et al., 2013a, 2013b). In short, the collected BAL fluid was placed on ice until BAL fluid cells were isolated by centrifugation at 400 x *g* for 10 min at 4 °C. The cells were re-suspended in 100 μL HAM's F12 medium (with 1% penicillin-streptomycin, 1% L-glutamine and 10% foetal bovine serum (FBS)). Next, 40 μL of the cell suspension was mixed with 60 μL freezing medium (HAM's F12 medium with 1% penicillin-streptomycin, 1% L-glutamine, 10% FBS and 10% dimethyl sulphoxide (DMSO)) and gently frozen at − 20 °C and subsequently transferred to − 80 °C until comet analysis. Lung and liver were recovered from the mice and samples were cut (~20–40 mg, 3 ×3 ×3 mm), transferred to NUNC cryotubes, snap-frozen in liquid N_2 and stored at − 80 °C until comet analysis.

All samples from all animals were thus frozen down and stored before the comet analyses were conducted on all samples on the same day of analysis. For the comet assay, the BAL cells were thawed at 37 °C, immediately embedded in 0.7% agarose, and kept on ice before being loaded onto Trevigen Comet Slides (Trevigen, Gaithersburg, MD, USA). Frozen lung and liver samples were pressed through a stainless steel cylindrical sieve (diameter 0.5 cm, mesh size 0.4 mm) into 0.5–2 mL ice-cold Merchant's medium (0.14 M NaCl, 1.47 mM KH_2PO_4, 2.7 mM KCl, 8.1 mM Na_2HPO_4, 10 mM Na_2EDTA, pH 7.4) and rapidly placed on ice until being embedded in 0.7% agarose and loaded onto Trevigen Comet Slides.

The slides were incubated overnight with 4 °C cold lysing buffer (2.5 M NaCl, 10 mM Tris, 100 mM sodium-ethylenediaminetetraacetic acid (EDTA), 1% sodium sarcosinate, 10% DMSO, 1% Triton X-100, pH 10). The slides were then rinsed for 5 min in cold electrophoresis buffer, and then for 35 min alkaline treated with ice-cold electrophoresis buffer directly in the electrophoresis chamber (0.3 M NaOH, 1 mM sodium-EDTA, pH 13.2). Electrophoresis conditions were 38 V (1.2 V/cm) for 25 min. After the run, the slides were rinsed in neutralisation buffer (0.4 M Tris, pH 7.5) 2 × 5 min, and treated for 5 min with 96% ethanol followed by incubation for 15 min at 45 °C. The cell nuclei were stained with SYBR® Green in TE buffer (10 mM Tris–HCl, 1 mM EDTA, pH 7.6). Automatic scoring was done with the IMSTAR PathFinder system (P Jackson et al., 2013a, 2013b). DNA strand breaks were evaluated as a percentage of DNA in the comet tail. Negative and positive controls for comet assay performance, A549 cells exposed to 0 or 30 μM H_2O_2 (30 min at 4 °C), respectively, were included on all slides. The negative A549 control furthermore allows comparison to other studies done in our lab.

2.5. Production of reactive oxygen species (ROS)

Using the 2′− 7′-dichlorodihydro-fluorescein diacetate ($DCFH_2$-DA) oxidation test, the production of ROS by tungsten was quantified as described previously (Danielsen et al., 2020). Briefly, Hank's balanced salt solution (HBSS) was used to prepare a particle stock suspension with a concentration of 1.35 mg tungsten/mL. The suspension was sonicated on ice for 16 min, with an amplitude of 10% using an S-450D Branson Sonifier (Branson Ultrasonics Corp., USA) The sonifier delivers 7.3 Watts at this amplitude (Booth and Jensen, 2015). HBSS was used to prepare dilutions from the stock suspension in the following concentrations: 0, 1.1, 2.1, 4.2, 8.4, 16.9, 33.8, 67.5, and 101.3 μg/mL. $DCFH_2$-DA was deacetylated to $DCFH_2$ by 0.01 M NaOH, for 30 min at room temperature in the dark, and then diluted with HBSS and kept in the dark. A 96-well plate was loaded with particle dilutions, then $DCFH_2$, in triplicates; plates were then incubated for 3 h at 37 ºC. Using a 1420 Victor^2 multilabel counter (Perkin Elmer, Denmark), the fluorescence of the formed 2′− 7′-dichlorofluorescein (DCF) was measured at wavelengths of 490 nm for the excitation and 520 nm for the emission. The test was done twice. Due to its well-known high ROS generation, carbon black was included as a reference material (Boyles et al., 2022). The slopes from the linear range of the dose-response curves for carbon black and tungsten (0–22.5 μg/mL for carbon black and 0–45 μg/mL for tungsten) were used to assess the ROS production.

2.6. Histopathology, testosterone plasma concentration and sperm production

Livers and kidneys from High exposure animals were fixed in 4% formalin for at least 24 h, and next trimmed, dehydrated, and paraffin-embedded. Sections, 2–2.5 μm, were cut on a microtome, placed on microscope slides and stained with haematoxylin and eosin (H&E) stain (Histolab Products AB, Askim, Sweden). Next, the sections were evaluated for histopathological changes under a light microscope.

Mice were further assessed for effects on indicators of reproductive function: testosterone was measured using an ELISA kit (Biovendor,

Brno, Czech Republic Prod. No. RTC001R) that was validated previously in our lab (results not shown), according to the manufacturer's protocol. The detection limit was 0.066 ng/mL. The daily sperm production per testicle and sperm count per gram of testicular parenchyma (SC/g) was determined next. A previously validated protocol for mice was adopted for this study (Kyjovska et al., 2013). Shortly, the left testicle was excised at necropsy and stored at − 80°C until analysis. A shallow longitudinal incision facilitated the removal of the tunica albuginea. The testicle was then weighed and transferred to a 50 mL Eppendorf tube with 4 mL 0.05% Triton X-100 homogenisation buffer (Sigma®, Germany), homogenized for 5 min using an IKA ULTRA TURRAX ® T25 disperser S25N-10 G, and placed on ice for approximately 30 min. Then 200 µL of 0.04% Trypan blue solution (Sigma®, Germany) was added to an equal volume of tissue homogenate. The mixture was suspended with a pipette and loaded onto a Double Neubauer Improved haemocytometer (depth 0.1 mm) in a humidity chamber. After at least 2 min, the homogenisation-resistant spermatids (stages 14–16) were counted using a light microscope (Olympus BX43) at 40x magnification. Each sample was counted in quadruplicate (six samples in duplicate only) and averaged. Next, daily sperm production was calculated by dividing total sperm count by 4.84; the time divisor value that corresponds to the number of days mouse spermatids spend in spermatogenic stages 14–16 (Oakberg, 1956). The sperm count (SC)/g testicular tissue was calculated by dividing the total sperm count by testicular weight. Finally, relative testicle weight was achieved by dividing the testicle weight by body weight.

2.7. Statistics

We calculated the statistics using the Graph Pad Prism software package 7.02 (Graph Pad Software Inc., La Jolla, CA, USA). First, we tested the data for normality using the Shapiro-Wilk test. The ANOVA test is relatively robust to moderate departures from normality (Petrie and Sabin, 2005). Hence ANOVA was applied, except if the P value of the Shapiro-Wilk test was very low ($P < 0.001$). Second, the ANOVA is somewhat sensitive to differences in standard deviation. Thus, ANOVA was not calculated if standard deviations were very different in the Brown-Forsythe tests ($P < 0.001$). In case we observed the described deviations in normality or in standard deviations, the non-parametric Kruskall-Wallis test was calculated instead of the ANOVA test. To determine differences between the control and treated groups, we employed the following post-tests: For the ANOVA we calculated Holm-Sidak's multiple comparisons test (Holm, 1979) For the Kruskall-Wallis test we calculated Dunn's multiple comparisons test.

3. Results

3.1. Tungsten properties

The specific surface area of the tungsten powder was 1.382 m^2/g. The total pore volume (at p/p0 = 0.99000) was 0.005 cm^3 /g, and the average pore diameter (4 V/A) was 14.9 nm. Moreover, HK/SF micropore analysis (<2 nm) gave a micropore volume of 0.001 cm^3 /g; a most frequent pore diameter of 1.013 nm; and a median pore diameter of 0.74 nm.

The normalised aerodynamic particle number size distribution of the aerosolised tungsten is shown in Supplemental Materials Fig. S1, and was found to be bimodal. The particle number size distribution was fitted with a lognormal size distribution, and had a lower mode of 0.6 µm and a higher mode of 1.8 µm. The lower mode was fully within the respirable range of mice (<1 µm) (Asgharian et al., 2014), while the higher mode was partially within the respirable range of mice, with sizes larger than the respirable range in an upper tail (Supplemental Materials Fig. S1). The particle size distribution was consistent over all concentrations. The final determined mass concentrations in the inhalation chamber were 9 ± 6 (Low, mean±SD), 23 ± 7 (Mid) or 132 ± 56 mg/m^3 (High).

The estimated alveolar deposition was in the MPPD model calculated to 0.0 (control), 0.89 (Low), 2.28 (Mid), and 13.1 µg/mouse (High), based on an estimated pulmonary deposited mass rate of 0.000221 (µg*m^3/(min*mg)) and the applied exposure levels, time and days of exposure.

S.

3.2. Body weight gain and clinical appearance

The mouse in the pilot study, which was given High exposure (132 mg/m^3), showed no clinical signs of toxicity. In the main study, there was a decrease in end body weight for High exposure as compared to controls (data not shown). Yet we saw no changes in body weight during the exposure period (Fig. 1), suggesting differences in start body weight were a possible explanation of the lower end-body-weight for High exposure. Notably, two animals at Low exposure were killed prematurely due to a loss of 16% and 17% of their initial body weight. As other animals in this group had no reduction in body weight, this did not translate into overall lower body weight gain in this group. We saw no clinical signs of toxicity such as immobility, piloerection, or hunched posture in any of the groups during the study. The two prematurely killed animals were removed from the dataset except in Fig. 1.

3.3. BAL fluid cellularity including pulmonary inflammation and BAL fluid biochemistry

We found no indications of lung inflammation measured as neutrophil numbers in BAL fluid, nor did we see changes in total cell numbers, macrophages, lymphocytes, or epithelial cells in this compartment (Supplemental Materials Fig. S2). Particles were noted in the BAL fluid in 5 of 6 evaluated samples at High Exposure, while this phenomenon was only seen in 2 of 8 samples from Mid exposure, and in none of the other groups (data not shown). Particles were seen in macrophages in all three tungsten exposed groups as black particles likely consisting of tungsten. What appeared as blue particles were seen in all groups including in controls (Supplemental Materials Fig. S3). LDH and total protein in BAL fluid were similar in the control and exposed groups (data not shown).

3.4. Genotoxicity and ROS production

Genotoxicity was determined with the comet assay as the percentage of DNA in the comet tail. The level of DNA strand breaks was elevated in

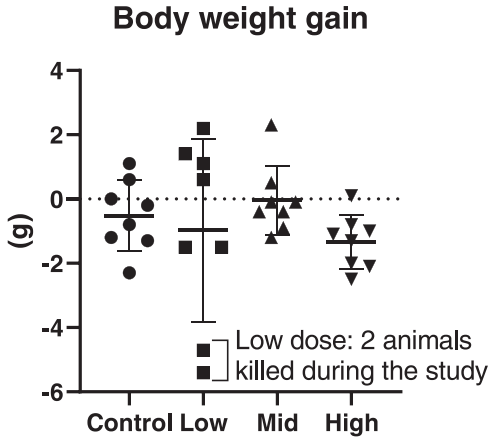

Fig. 1. Body weight gain at the end of the 15-day experimental period. The horizontal lines represent mean values and the bars one standard deviation (SD). Two animals in the Low dose group were killed due to weight losses of 16% and 17%.

BAL fluid cells at Low and High exposure, but not at Mid exposure (Fig. 2 and Supplemental Materials Figs. S4 and S5). We saw no increase in genotoxicity in lung and liver tissue (Fig. 2). Concerning acellular ROS production, the $DCFH_2$-DA assay results showed a dose-dependent increase in ROS production for tungsten (Fig. 3). By mass, tungsten had a lower ability to produce ROS (a slope of 319 arbitrary units/μg/mL) than carbon black (3083 arbitrary units/μg/mL). The initial slope of tungsten was 10 times smaller than that of carbon black by mass. For ROS production normalised to surface area, tungsten exhibited a slope of 23083 arbitrary units/cm^2/mL, while the slope of carbon black was 1043 arbitrary units/cm^2/mL (Supplemental Materials Fig. S6).

3.5. Histopathology, testosterone and sperm counts

We observed no pathological effects in the liver and kidney (Supplemental Materials Figs. S7 and S8). The testosterone plasma concentration was decreased at Low dose only (Fig. 4). No effects were seen on sperm numbers, neither assessed as daily sperm production nor as sperm numbers per gram of testicle (Fig. 4, and Supplemental Materials Fig. S9).

4. Discussion

4.1. Tungsten inhalation did not affect body weight, pulmonary inflammation or pathology in the liver and kidney

We saw no effect on body weight at tungsten exposure levels up to 132 mg/m^3. To our knowledge, there are no toxicity data on pure tungsten inhalation in the peer-reviewed literature (Hadrup et al., 2022). Concerning other tungsten substances, no effect on body weight development was observed in Syrian hamsters inhaling tungsten trioxide nanoparticles (diameter ca. 100 nm) at 5 or 10 mg WO_3/m^3 (=4 or 8 mg W/m^3), 4 h/day for 4 or 8 days showed (Prajapati et al., 2017) nor in rats after inhalation of tungsten blue oxide at the relatively high mass concentrations of ~63, 257 or 514 mg W/m^3, 6 h/day for 28 days (Rajendran et al., 2012). Overall, our $NOAEC_{body\ weight}$ of 132 mg W/m^3 is in line with the limited literature on other tungsten substances.

We saw no effect on pulmonary inflammation measured as neutrophil numbers in BAL fluid. One intratracheal instillation study in rats with 20 mg/kg bw of pure tungsten (1–5 μm in diameter) reported no effect on this endpoint (Roedel et al., 2012), while we have not identified studies assessing neutrophil numbers in BAL fluid after inhalation exposure to pure tungsten.

In the aforementioned study of tungsten blue oxide, neutrophils were increased in blood at the highest dose only (514 mg W/m^3), while increases in alveolar pigmented macrophages, as well as foamy macrophages, were observed at all three doses (≥63 mg W/m^3) (Rajendran et al., 2012). The study in Syrian hamsters on tungsten trioxide nanoparticles (102 nm) had a $NOAEC_{BAL\ neutrophils}$ of 5 mg WO_3/m^3 (=4 mg W/m^3), and a LOAEC of 10 mg WO_3/m^3 (=8 mg W/m^3) (Prajapati et al., 2017). That study did not report the specific surface area of the particles, but nanosize generally means significantly larger specific surface area per mass unit as compared with micro-sized particles. Though, on the other hand, tungsten has a density of 19.3 g/cm^3, leading to a relatively low BET value as compared to other materials.

The particle used in our study has a reported size of < 1 μm, and a specific surface area of 1.4 m^2/g. We estimated the alveolar deposition to be 0.89 (Low), 2.28 (Mid), and 13.1 (High) μg tungsten/mouse. The total surface area in lung of the retained particles was estimated to be 0.012, 0.031, and 0.18 cm^2/mouse, for Low, Mid and High exposure, respectively. Retained surface area has been identified as an important predictor of pulmonary inflammation (Cosnier et al., 2021; Danielsen et al., 2020; Schmid and Stoeger, 2016), with a reported threshold for neutrophil influx of 20 cm^2/mouse for carbon black particles (Stoeger et al., 2006). The lack of pulmonary inflammation in the present study is therefore consistent with the estimated low deposited surface area of the employed tungsten (0.18 cm^2/mouse for High exposure).

We can also compare the effects of tungsten to those of other metals, for example silver, the pulmonary toxicity of which we recently reviewed (Hadrup et al., 2020). Inhalation of silver nanoparticles in rats has shown increased neutrophils in BAL fluid at mass concentrations as low as 0.043 and 0.18 mg/m^3 (Braakhuis et al., 2016, 2014), suggesting that some metals can induce inflammation already at low exposure levels, albeit this might in part be explained by higher specific surface area and solubility, and hence release of ions, of the silver particles (Hadrup et al., 2020). TiO_2 particles with a specific surface area similar to that of the tungsten used in the current work (2 vs. 1.4 m^2/g, respectively) did also not increase neutrophils in BAL fluid of mice inhaling the highest tested mass concentration (10 mg/m^2) for 2 h per day, 4 days/week for 4 weeks (Rossi et al., 2010), nor at 16 mg/m^3 for the same species for 1 h/day, 4 days/week for 4 weeks (Leppänen et al., 2015).

We observed no pathological effects in the liver and kidney, suggesting no severe toxicity to these organs, likely reflecting that although the tungsten particles had sizes < 1 μm, only low levels of translocation is expected, since the lung burden of tungsten was low in the current study and since translocation is highly size-dependent (Stone et al., 2017). Yet in other studies, tungsten does pass the kidney, as it is reported to be present in human urine in workers exposed to tungsten during the production of diamond tools (Goldoni et al., 2004). Tungsten was also shown in urine and in the kidneys, among other organs, in rats after inhalation of sodium tungstate ($Na_2^{188}WO_4$) at 256 mg W/m^3 for 90 min (Radcliffe et al., 2010). Apparently, no studies have reported on the presence of tungsten in the liver (Hadrup et al., 2022).

4.2. Tungsten inhalation and genotoxicity

We observed genotoxic effects in BAL fluid cells at Low and High exposure, but not at Mid exposure. Thus, we did not see dose-dependency. One explanation for the lack of effect at Mid exposure, could be that this group had two weekends to recover during their 10-day exposure period, compared to only one weekend in the other groups. Another possibility is that there is a non-monotonous dose-response for tungsten on this endpoint, e.g. based on upregulation of protective mechanisms at Mid exposure, which are overwhelmed at High exposure. A third aspect is we often see non-dose related effects with this assay (Hadrup et al., 2021b, 2021a, 2019; Kyjovska et al., 2015), an explanation for this is the assay is not well-suited for the detection of dose-related effects of particle exposure, due to a limited dynamic range.

We recently reviewed the literature on the genotoxicity of tungsten (Hadrup et al., 2022). Notably, no relevant studies were using pulmonary exposure, but for other exposure routes there were. One study actually supports a non-dose-dependent effect of tungsten on genotoxicity. Kelly et al. (2013) dosed mice with tungsten for 16 weeks via the drinking water (2.2, 30 or 150 mg W/kg bw/day). DNA strand breaks were measured in bone marrow cells after 1, 4, 8, 12, or 16 weeks. Only after 4 weeks were strand breaks increased at all three dose levels; there was no effect at the highest dose level at earlier sampling times. In another study, Guilbert and colleagues exposed mice to tungsten at 3.75 or 50 mg W/kg bw/day for 8 weeks via drinking water, and found dose-dependent genotoxicity in bone marrow cells with the comet assay (Guilbert et al., 2011). Chinde and co-workers tested tungsten trioxide nano- and microparticles by oral gavage of rats at single doses of 80, 400, or 800 mg W/kg bw. At the highest dose level of nanoparticles, genotoxicity was increased in the micronucleus test (bone marrow cells) and comet assay (BAL blood lymphocytes and liver cells); while their microsized counterparts had no effect (Chinde et al., 2017).

Overall, oral studies provide evidence of genotoxicity of tungsten observed as DNA strand breaks and clastogenic effects. Tungsten in combination with cobalt shows genotoxicity after inhalation, and the potential for genotoxicity in vivo is supported by numerous in vitro

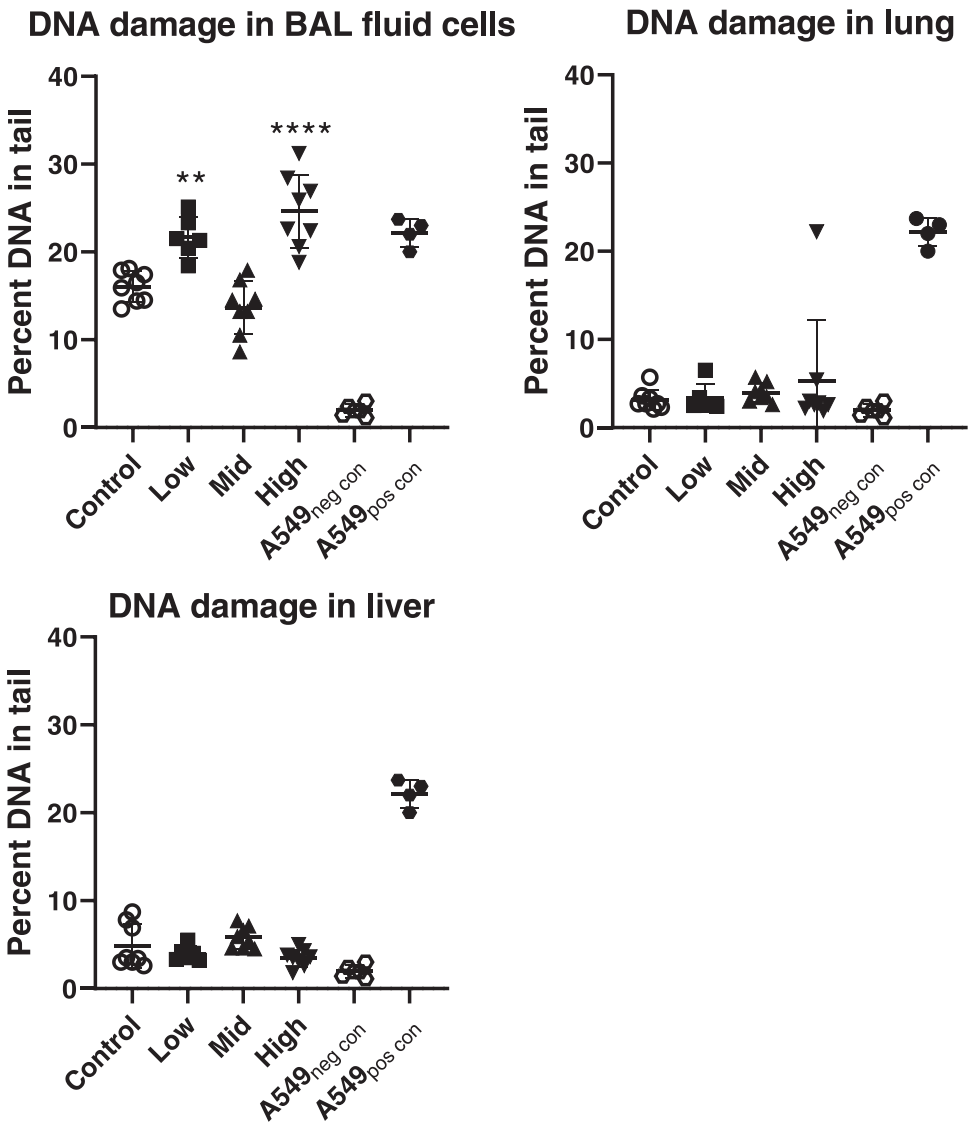

Fig. 2. Genotoxicity in BAL fluid cells, lung and liver tissue. Genotoxicity was determined as the percentage of DNA in the tail in the comet assay. $A549_{neg\ con}$ designates A549 cells as negative controls and $A549_{neg\ con}$ designates H_2O_2-treated A549 cells as positive controls. The horizontal lines show mean levels and the bars show one SD. **** and * designate P values of < 0.001 or < 0.05, respectively, of one-way ANOVA with the Holm-Sidak's multiple comparisons test. The negative and positive controls were not included in the statistical testing.

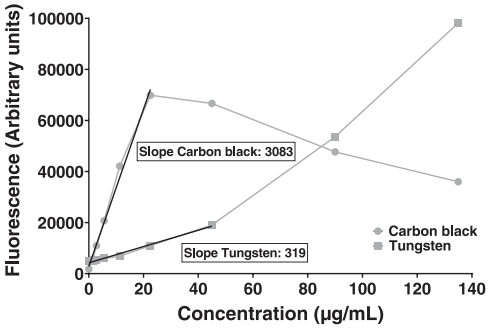

Fig. 3. In vitro ROS production normalised to mass from tungsten and carbon black Printex 90. Values are shown as mean arbitrary units of three replicates, within one experiment. Slopes for each dose-response curve were calculated using linear regression, in the range of 0–22.5 µg/mL for carbon black and 0–45 µg/mL for tungsten.

studies (Hadrup et al., 2022).

Genotoxicity may lead to cancer. Tumour numbers were however not elevated in rats exposed to tungsten via drinking water for their entire life (Schroeder and Mitchener, 1975). Yet a carcinogenic potential of tungsten was observed in rats implanted intramuscularly with tungsten alloy pellets (91% tungsten, 6% Ni, and 3% Co), resulting in the development of tumours in all rats (pleomorphic rhabdomyosarcomas which rapidly developed lung metastasis). Nonetheless, that effect may also be caused by the nickel or cobalt content (Kalinich et al., 2005).

Tungsten belongs to the same elemental group (VIB) in the Periodic Table of the Elements as molybdenum and chromium. We recently investigated molybdenum in a similar setup and observed genotoxicity in BAL cells (Sørli et al., 2023), and hexavalent chrome is a known human carcinogen (IARC, 1990).

The genotoxicity observed in our study occurred in absence of inflammation, indicating a primary genotoxic effect. Both primary (directly on the DNA[1]) and secondary genotoxicity (DNA damage via other molecules) have been suggested to contribute to particle-induced carcinogenesis (Nymark et al., 2021). In comparison to carbon black Printex 90, tungsten had only limited ROS production per mass unit in the acellular test (Fig. 3). In the Supplemental Materials, we describe several articles that suggest carbon black induces genotoxicity at similar mass concentrations as the one used for tungsten in the current study (Gallagher et al., 2003; Jackson et al., 2012; Saber et al., 2005; Wolff

[1] We consider genotoxicity via ROS production to be primary genotoxicity

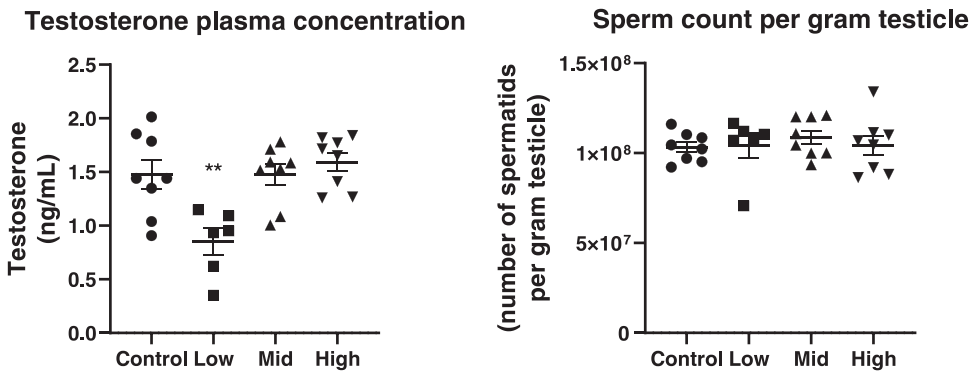

Fig. 4. Testosterone in plasma and sperm count after inhalation of tungsten. The horizontal lines show mean levels and the bars show one SD. * * designates a P value of < 0.01, one-way ANOVA with the Holm-Sidak's multiple comparisons test.

et al., 1990) (Supplemental Materials). The observation of genotoxicity at 9 and 132 mg W/m^3 and the limited ROS activity of our tungsten particles in comparison to carbon black nanoparticles, could at first thought suggest that ROS production of tungsten is not a major cause of the genotoxicity. Nonetheless, the tungsten particle had a specific surface area of 1.4 m^2/g, whereas the carbon black Printex 90 has a specific surface area of ~300 m^2/g. If ROS generation is normalised to surface area, the tungsten particles have a higher ROS generation potential than carbon black particles (Supplemental Materials Fig. S4). Hence, we cannot rule out that ROS contributes to the observed genotoxicity.

The estimated deposited lung burden of tungsten was very modest, due to the large aerosolized particle size. Thus, we would expect that the vast majority of the particles were taken up by macrophages, at least at the lowest exposure levels. In agreement with this, particles were observed outside macrophages mainly at High exposure and to a lesser extent at Mid exposure. This differential particle distribution may be one of the reasons why we only observed genotoxicity in BAL cells, as these would have been the most exposed cells. However, it is possible that longer follow-up would allow the tungsten particles to redistribute leading to particle exposure of other cell types.

Our data showing a genotoxic potential of tungsten after inhalation are in line with the very few published studies. To the best of our knowledge, this study is the first to report genotoxicity following inhalation exposure. Genotoxicity was observed at Low exposure suggesting a LOAEC of 9 mg/m^3 for the 45 min exposure, corresponding to 0.84 mg/m^3 for an 8-hour working day. A no-adverse-effect concentration could not be established. ROS production per mass unit is low due to the relatively large particle size, but the ROS generation normalised to surface area is high (Supplemental Materials Fig. S4). It is therefore possible that generated ROS contributed to the observed genotoxicity. Finally, while the comet assay allows us to screen specific cells and tissues that are among the first to interact with the MoS_2 particles upon inhalation, we note that other assays e.g. micronuclei detection in erythrocytes or chromosomal aberrations in bone marrow cells could have strengthened the conclusion on genotoxicity.

4.3. Sperm counts

There was no effect on sperm counts in the current study. Nonetheless, we found a decreased testosterone concentration at the lowest dose level. This effect did not translate into changes in sperm production, maybe because the testosterone was reduced for too short a period to affect spermatogenesis, as described by (Adler, 1996). The finding of a non-monotonous dose-response on this endpoint could reflect that the body, at higher doses, has some compensatory mechanism at play to increase testosterone levels, either via production or elimination regulation.

Despite that a large number of metals and metalloids have been studied for possible effects on various reproductive parameters in males, data on reproductive toxicity of tungsten is scarce. We only identified a single study on male reproductive toxicity of tungsten; a U.S. cohort study of 413 men of reproductive age performed between 2005 and 2009. The study evaluated the effects of 15 creatinine-adjusted metal (loid)s on semen quality. Tungsten was detected in 59% of the participants but was not significantly associated with any of the assessed reproductive parameters (Branch et al., 2021).

Previous studies indicate that exposure to other metal(loid)s can reduce semen quality and disrupt reproductive function. Hence, metal (loid)s can affect the reproductive system directly by inducing tissue damage, and indirectly by interfering with the production and secretion of hormones (Branch et al., 2021). Another study implied that iron and copper can compromise the spermatogenic cycle and induce oxidative damage to the testicular tissue and spermatozoa, when accumulating in high quantities in the human body (Tvrda et al., 2015). Furthermore, cadmium and lead have been negatively associated with sperm concentration and semen volume in humans (Hernández-Ochoa et al., 2005; Jeng et al., 2014; Li et al., 2016) and a plethora of reproductive effects in animals, including reduced spermatogenesis and spermatocyte DNA damage (Blanco et al., 2010; Kotsonis and Klaassen, 1977; Nava-Hernández et al., 2009). Silver, aluminium, and molybdenum trioxide have also demonstrated toxicity to spermatogonian stem cells in mice (Hjollund et al., 1998). Rats exposed to nickel exhibited decreased sperm count and motility, altered steroidogenesis and a combination of high testicular lipid peroxidation and reduced antioxidant enzyme activity (Das and Dasgupta, 2002; Gupta et al., 2007).

In the present study, exposure to tungsten within the tested range (9, 23 and 132 mg/m^3) did not affect the daily sperm production and absolute and relative testicle weights. However, it should be emphasized that the period of exposure did not cover the entire spermatogenic cycle of mice (Adler, 1996). Since the method for estimating daily sperm production only takes into account spermatids in their latest stages (14–16), these would not have been exposed to tungsten during the entire period of differentiation. Furthermore, oxidative stress is a commonly proposed mechanism of action for conditions associated with male infertility, and high levels of ROS impair sperm quality by increasing the oxidation of DNA, proteins and lipids (De Luca et al., 2021). It is crucial that future studies investigate the effects of longer-term exposures covering the entire period of spermatogenesis and preferentially include biomarkers of oxidative stress.

5. Conclusions

Following inhalation of tungsten in mice, we here report genotoxicity in BAL fluid cells at Low and High exposure (9 and 132 mg/m^3). Genotoxicity was observed in the absence of pulmonary inflammation, indicating a primary genotoxic effect. The studied tungsten particles have a relatively low ROS potential per mass unit, but a relatively high ROS potential normalised to specific surface area. Therefore, we cannot

rule out that generated ROS could have contributed to the observed genotoxicity. Plasma testosterone was decreased at the Low exposure only, and sperm counts were unaffected. Based on the genotoxicity seen at the lowest exposure, a LOAEC of 9 mg tungsten/m^3 could be suggested. Normalising the exposure to an 8-hour working day, this corresponds to 0.84 mg/m^3. A no-adverse-effect concentration could not be established. Yet noting the only other effect observed was a decrease in testosterone at this level, we suggest that additional studies are needed to firmly set dose descriptors for this metal after inhalation. Nonetheless, the genotoxic effect seen in the current study is consistent with the literature, pointing to a genotoxic potential of this metal.

CRediT authorship contribution statement

Jorid B. Sørli: Conceptualization, Investigation, Formal analysis, Visualization, Writing – review & editing, Funding acquisition. **Alexander C.Ø. Jensen:** Investigation, Formal analysis, Writing – review & editing. **Alicja Mortensen:** Investigation, Formal analysis, Visualization, Writing – review & editing. **Józef Szarek:** Investigation, Formal analysis, Visualization, Writing – review & editing. **Eleni Chatzigianelli:** Investigation, Formal analysis, Writing – review & editing. **Claudia A.T. Gutierrez:** Investigation, Formal analysis, Visualization, Writing – review & editing. **Nicklas R. Jacobsen:** Investigation, Formal analysis, Writing – review & editing. **Sarah S. Poulsen:** Investigation, Writing – review & editing. **Iosif Hafez:** Investigation, Formal analysis, Writing – review & editing. **Charis Loizides:** Investigation, Formal analysis, Writing – review & editing. **George Biskos:** Investigation, Formal analysis, Writing – review & editing. **Karin S. Hougaard:** Formal analysis, Writing – review & editing. **Ulla Vogel:** Formal analysis, Writing – review & editing, Funding acquisition. **Niels Hadrup:** Conceptualization, Investigation, Formal analysis, Visualization, Writing – original draft, Writing – review & editing, Project administration, Funding acquisition.

Declaration of Competing Interest

The authors declare the following financial interests/personal relationships which may be considered as potential competing interests: Niels Hadrup reports financial support was provided by The Danish Working Environment Research Fund. Ulla Vogel reports financial support was provided by The Danish Government.

Data Availability

Data will be made available on request.

Acknowledgements

The excellent technical assistance of Eva Terrida, Michael Guldbrandsen, Noor Irmam, Anne Abildtrup, Yasmin Akhtar, Signe Hjortkær Nielsen and Bianca Xuan Nguyen Larsen is greatly appreciated. This work was supported by a grant from the Danish Working Environment Research Fund [grant number Sikker-Motor 29-2019-09] and FFIKA, Focused Research Effort on Chemicals in the Working Environment, from the Danish Government.

Appendix A. Supporting information

Supplementary data associated with this article can be found in the online version at doi:10.1016/j.etap.2023.104074.

References

Adler, I.-D., 1996. Comparison of the duration of spermatogenesis between male rodents and humans. Mutat. Res. Mol. Mech. Mutagen. 352, 169–172. https://doi.org/10.1016/0027-5107(95)00223-5.

Arbejdstilsynet, 2023. Bilag 2 - Grænseværdier for luftforureninger m.v. [WWW Document]. URL ⟨https://at.dk/regler/bekendtgoerelser/graensevaerdier-stoffer-materialer-1054/bilag-2/⟩.

Asgharian, B., Price, O.T., Oldham, M., Chen, L.-C., Saunders, E.L., Gordon, T., Mikheev, V.B., Minard, K.R., Teeguarden, J.G., 2014. Computational modeling of nanoscale and microscale particle deposition, retention and dosimetry in the mouse respiratory tract. Inhal. Toxicol. 26, 829–842. https://doi.org/10.3109/08958378.2014.935535.

Blanco, A., Moyano, R., Molina López, A.M., Blanco, C., Flores-Acuña, R., García-Flores, J.R., Espada, M., Monterde, J.G., 2010. Preneoplastic and neoplastic changes in the Leydig cells population in mice exposed to low doses of cadmium. Toxicol. Ind. Health 26, 451–457. https://doi.org/10.1177/0748233710371111.

Booth, A., Jensen, K., 2015. NANoREG D4.12 SOP Probe Sonicator Calibration for ecotoxicological testing.

Boyles, M., Murphy, F., Mueller, W., Wohlleben, W., Jacobsen, N.R., Braakhuis, H., Giusti, A., Stone, V., 2022. Development of a standard operating procedure for the DCFH 2 -DA acellular assessment of reactive oxygen species produced by nanomaterials. Toxicol. Mech. Methods 32, 439–452. https://doi.org/10.1080/15376516.2022.2029656.

Braakhuis, H.M., Gosens, I., Krystek, P., Boere, J.A., Cassee, F.R., Fokkens, P.H., Post, J. A., van, L.H., Park, M.V., 2014. Particle size dependent deposition and pulmonary inflammation after short-term inhalation of silver nanoparticles. Part Fibre Toxicol. 11, 49.

Braakhuis, H.M., Giannakou, C., Peijnenburg, W.J., Vermeulen, J., van, L.H., Park, M.V., 2016. Simple in vitro models can predict pulmonary toxicity of silver nanoparticles. Nanotoxicology 10, 770–779.

Branch, F.M., Perry, M.J., Chen, Z., Louis, G.M.B., 2021. Metal(loid)s and human semen quality: the LIFE study. Reprod. Toxicol. 106, 94–102. https://doi.org/10.1016/j.reprotox.2021.10.006.

Chinde, S., Dumala, N., Rahman, M.F., Kamal, S.S.K., Kumari, S.I., Mahboob, M., Grover, P., 2017. Toxicological assessment of tungsten oxide nanoparticles in rats after acute oral exposure. Environ. Sci. Pollut. Res. 24, 13576–13593. https://doi.org/10.1007/s11356-017-8892-x.

Cosnier, F., Seidel, C., Valentino, S., Schmid, O., Bau, S., Vogel, U., Devoy, J., Gaté, L., 2021. Retained particle surface area dose drives inflammation in rat lungs following acute, subacute, and subchronic inhalation of nanomaterials. Part. Fibre Toxicol. 18, 29. https://doi.org/10.1186/s12989-021-00419-w.

Danielsen, P.H., Knudsen, K.B., Štrancar, J., Umek, P., Koklič, T., Garvas, M., Vanhala, E., Savukoski, S., Ding, Y., Madsen, A.M., Jacobsen, N.R., Weydahl, I.K., Berthing, T., Poulsen, S.S., Schmid, O., Wolff, H., Vogel, U., 2020. Effects of physicochemical properties of TiO2 nanomaterials for pulmonary inflammation, acute phase response and alveolar proteinosis in intratracheally exposed mice. Toxicol. Appl. Pharmacol. 386, 114830 https://doi.org/10.1016/j.taap.2019.114830.

Das, K.K., Dasgupta, S., 2002. Effect of nickel sulfate on testicular steroidogenesis in rats during protein restriction. Environ. Health Perspect. 110, 923–926. https://doi.org/10.1289/ehp.02110923.

De Luca, M.N., Colone, M., Gambioli, R., Stringaro, A., Unfer, V., 2021. Oxidative stress and male fertility: role of antioxidants and inositols. Antioxidants 10. https://doi.org/10.3390/antiox10081283.

Gallagher, J., Sams, R., Inmon, J., Gelein, R., Elder, A., Oberdorster, G., Prahalad, A.K., 2003. Formation of 8-oxo-7,8-dihydro-2′-deoxyguanosine in rat lung DNA following subchronic inhalation of carbon black. Toxicol. Appl. Pharmacol. 190, 224–231.

Goldoni, M., Catalani, S., De Palma, G., Manini, P., Acampa, O., Corradi, M., Bergonzi, R., Apostoli, P., Mutti, A., 2004. Exhaled breath condensate as a suitable matrix to assess lung dose and effects in workers exposed to cobalt and tungsten. Environ. Health Perspect. 112, 1293–1298. https://doi.org/10.1289/ehp.7108.

Graczyk, H., Lewinski, N., Zhao, J., Concha-Lozano, N., Riediker, M., 2016. Characterization of tungsten inert gas (TIG) welding fume generated by apprentice welders. Ann. Occup. Hyg. 60, 205–219. https://doi.org/10.1093/annhyg/mev074.

Guilbert, C., Kelly, A.D.R., Petruccelli, L.A., Lemaire, M., Mann, K.K., 2011. Exposure to tungsten induces DNA damage and apoptosis in developing B lymphocytes. Leukemia 25, 1900–1904. https://doi.org/10.1038/leu.2011.160.

Gupta, A.Das, Dhundasi, S.A., Ambekar, J.G., Das, K.K., 2007. Effect of 1-ascorbic acid on antioxidant defense system in testes of albino rats exposed to nickel sulfate. J. Basic Clin. Physiol. Pharmacol. 18. https://doi.org/10.1515/JBCPP.2007.18.4.255.

Hadrup, N., 2014. Evidence from pharmacology and pathophysiology suggests that chemicals with dissimilar mechanisms of action could be of bigger concern in the toxicological risk assessment of chemical mixtures than chemicals with a similar mechanism of action. Regul. Toxicol. Pharmacol. 69, 281–283. https://doi.org/10.1016/j.yrtph.2014.05.007.

Hadrup, N., Taxvig, C., Pedersen, M., Nellemann, C., Hass, U., Vinggaard, A.M., 2013. Concentration addition, independent action and generalized concentration addition models for mixture effect prediction of sex hormone synthesis in vitro. PLoS One 8, e70490. https://doi.org/10.1371/journal.pone.0070490.

Hadrup, N., Rahmani, F., Jacobsen, N., Saber, A., Jackson, P., Bengtson, S., A, W., Wallin, H., Halappanavar, S., Vogel, U., 2019. Acute phase response and inflammation following pulmonary exposure to low doses of zinc oxide nanoparticles in mice. Nanotoxicology. https://doi.org/10.1080/17435390.2019.1654004.

Hadrup, N., Sharma, A.K., Loeschner, K., Jacobsen, N.R., 2020. Pulmonary toxicity of silver vapours, nanoparticles and fine dusts: a review. Regul. Toxicol. Pharmacol. 115, 104690 https://doi.org/10.1016/j.yrtph.2020.104690.

Hadrup, N., Aimonen, K., Ilves, M., Lindberg, H., Atluri, R., Sahlgren, N.M., Jacobsen, N. R., Barfod, K.K., Berthing, T., Lawlor, A., Norppa, H., Wolff, H., Jensen, K.A., Hougaard, K.S., Alenius, H., Catalan, J., Vogel, U., 2021a. Pulmonary toxicity of synthetic amorphous silica - effects of porosity and copper oxide doping. Nanotoxicology 15, 96–113. https://doi.org/10.1080/17435390.2020.1842932.

Hadrup, N., Knudsen, K.B., Carriere, M., Mayne-L'Hermite, M., Bobyk, L., Allard, S., Miserque, F., Pibaleau, B., Pinault, M., Wallin, H., Vogel, U., 2021b. Safe-by-design strategies for lowering the genotoxicity and pulmonary inflammation of multiwalled carbon nanotubes: reduction of length and the introduction of COOH groups. Environ. Toxicol. Pharmacol. 87, 103702 https://doi.org/10.1016/j.etap.2021.103702.

Hadrup, N., Sørli, J.B., Sharma, A.K., 2022. Pulmonary toxicity, genotoxicity, and carcinogenicity evaluation of molybdenum, lithium, and tungsten: a review. Toxicology 467, 153098. https://doi.org/10.1016/j.tox.2022.153098.

Hernández-Ochoa, I., García-Vargas, G., López-Carrillo, L., Rubio-Andrade, M., Morán-Martínez, J., Cebrián, M.E., Quintanilla-Vega, B., 2005. Low lead environmental exposure alters semen quality and sperm chromatin condensation in northern Mexico. Reprod. Toxicol. 20, 221–228. https://doi.org/10.1016/j.reprotox.2005.01.007.

Hjollund, N.H.I., Bonde, J.P.E., Jensen, T.K., Ernst, E., Henriksen, T.B., Kolstad, H.A., Giwercman, A., Skakkebæk, N.E., Olsen, J., 1998. Semen quality and sex hormones with reference to metal welding. Reprod. Toxicol. 12, 91–95. https://doi.org/10.1016/S0890-6238(97)00156-1.

Holm, S., 1979. A simple sequentially rejective multiple test procedure. Scand. J. Stat. 6, 65–70.

Huaux, F., Lasfargues, G., Lauwerys, R., Lison, D., 1995. Lung toxicity of hard metal particles and production of interleukin-1, tumor necrosis factor-α, fibronectin, and cystatin-c by lung phagocytes. Toxicol. Appl. Pharmacol. 132, 53–62. https://doi.org/10.1006/taap.1995.1086.

IARC, 1990. Chromium, Nickel and Welding IARC Monographs on the Evaluation of Carcinogenic Risks to Humans Volume 49.

Jackson, P., Hougaard, K.S., Boisen, A.M., Jacobsen, N.R., Jensen, K.A., Moller, P., Brunborg, G., Gutzkow, K.B., Andersen, O., Loft, S., Vogel, U., Wallin, H., 2012. Pulmonary exposure to carbon black by inhalation or instillation in pregnant mice: effects on liver DNA strand breaks in dams and offspring. Nanotoxicology 6, 486–500.

Jackson, P., Pedersen, L.M., Kyjovska, Z.O., Jacobsen, N.R., Saber, A.T., Hougaard, K.S., Vogel, U., Wallin, H., 2013a. Validation of freezing tissues and cells for analysis of DNA strand break levels by comet assay. Mutagenesis 28, 699–707.

Jackson, Petra, Pedersen, L.M., Kyjovska, Z.O., Jacobsen, N.R., Saber, A.T., Hougaard, K.S., Vogel, U., Wallin, H., 2013b. Validation of freezing tissues and cells for analysis of DNA strand break levels by comet assay. Mutagenesis 28, 699–707. https://doi.org/10.1093/mutage/get049.

Jeng, H.A., Chen, Y.-L., Kantaria, K.N., 2014. Association of cigarette smoking with reproductive hormone levels and semen quality in healthy adult men in Taiwan. J. Environ. Sci. Health Part A 49, 262–268. https://doi.org/10.1080/10934529.2014.846195.

Kalinich, J.F., Emond, C.A., Dalton, T.K., Mog, S.R., Coleman, G.D., Kordell, J.E., Miller, A.C., McClain, D.E., 2005. Embedded weapons-grade tungsten alloy shrapnel rapidly induces metastatic high-grade rhabdomyosarcomas in F344 rats. Environ. Health Perspect. 113, 729–734. https://doi.org/10.1289/ehp.7791.

Kelly, A.D.R., Lemaire, M., Young, Y.K., Eustache, J.H., Guilbert, C., Molina, M.F., Mann, K.K., 2013. In vivo tungsten exposure alters B-cell development and increases DNA damage in murine bone marrow. Toxicol. Sci. 131, 434–446. https://doi.org/10.1093/toxsci/kfs324.

Klasson, M., Bryngelsson, I.-L., Pettersson, C., Husby, B., Arvidsson, H., Westberg, H., 2016. Occupational exposure to cobalt and tungsten in the swedish hard metal industry: air concentrations of particle mass, number, and surface area. Ann. Occup. Hyg. 60, 684–699. https://doi.org/10.1093/annhyg/mew023.

Kotsonis, F.N., Klaassen, C.D., 1977. Toxicity and distribution of cadmium administered to rats at sublethal doses. Toxicol. Appl. Pharmacol. 41, 667–680. https://doi.org/10.1016/S0041-008X(77)80020-3.

Kyjovska, Z.O., Boisen, A.M.Z., Jackson, P., Wallin, H., Vogel, U., Hougaard, K.S., 2013. Daily sperm production: Application in studies of prenatal exposure to nanoparticles in mice. Reprod. Toxicol. 36, 88–97. https://doi.org/10.1016/j.reprotox.2012.12.005.

Kyjovska, Z.O., Jacobsen, N.R., Saber, A.T., Bengtson, S., Jackson, P., Wallin, H., Vogel, U., 2015. DNA damage following pulmonary exposure by instillation to low doses of carbon black (Printex 90) nanoparticles in mice. Environ. Mol. Mutagen. 56, 41–49.

Lardot, C.G., Huaux, F.A., Broeckaert, F.R., Declerck, P.J., Delos, M., Fubini, B., Lison, D. F., 1998. Role of Urokinase in the Fibrogenic Response of the Lung to Mineral Particles. Am. J. Respir. Crit. Care Med. 157, 617–628. https://doi.org/10.1164/ajrccm.157.2.9707052.

Lasfargues, G., Lison, D., Maldague, P., Lauwerys, R., 1992. Comparative study of the acute lung toxicity of pure cobalt powder and cobalt-tungsten carbide mixture in rat. Toxicol. Appl. Pharmacol. 112, 41–50. https://doi.org/10.1016/0041-008X(92)90277-Y.

Lasfargues, G., Lardot, C., Delos, M., Lauwerys, R., Lison, D., 1995. The delayed lung responses to single and repeated intratracheal administration of pure cobalt and hard metal powder in the rat. Environ. Res. 69, 108–121. https://doi.org/10.1006/enrs.1995.1032.

Leppänen, M., Korpi, A., Yli-Pirilä, P., Lehto, M., Wolff, H., Kosma, V.-M., Alenius, H., Pasanen, P., 2015. Negligible respiratory irritation and inflammation potency of pigmentary TiO2 in mice. Inhal. Toxicol. 27, 378–386. https://doi.org/10.3109/08958378.2015.1056890.

Li, Y., Wu, J., Zhou, W., Gao, E., 2016. Association between environmental exposure to cadmium and human semen quality. Int. J. Environ. Health Res. 26, 175–186. https://doi.org/10.1080/09603123.2015.1061115.

Nava-Hernández, M.P., Hauad-Marroquín, L.A., Bassol-Mayagoitia, S., García-Arenas, G., Mercado-Hernández, R., Echávarri-Guzmán, M.A., Cerda-Flores, R.M., 2009. Lead-, cadmium-, and arsenic-induced DNA damage in rat germinal cells. DNA Cell Biol. 28, 241–248. https://doi.org/10.1089/dna.2009.0860.

Nymark, P., Karlsson, H.L., Halappanavar, S., Vogel, U., 2021. Adverse outcome pathway development for assessment of lung carcinogenicity by nanoparticles. Front. Toxicol. 3, 653386 https://doi.org/10.3389/ftox.2021.653386.

Oakberg, E.F., 1956. Duration of spermatogenesis in the mouse and timing of stages of the cycle of the seminiferous epithelium. Am. J. Anat. 99, 507–516. https://doi.org/10.1002/aja.1000990307.

Peão, M.N.D., Águas, A.P., de Sá, C.M., Grande, N.R., 1993. Inflammatory response of the lung to tungsten particles: An experimental study in mice submitted to intratracheal instillation of a calcium tungstate powder. Lung 171, 187–201. https://doi.org/10.1007/BF00203719.

Petrie, A., Sabin, C., 2005. Medical Statistics at a Glance, second ed. Blackwell Publishing Ltd.

Prajapati, M.V., Adebolu, O.O., Morrow, B.M., Cerreta, J.M., 2017. Original research: evaluation of pulmonary response to inhaled tungsten (IV) oxide nanoparticles in golden Syrian hamsters. Exp. Biol. Med. 242, 29–44. https://doi.org/10.1177/1535370216665173.

Radcliffe, P.M., Leavens, T.L., Wagner, D.J., Olabisi, A.O., Struve, M.F., Wong, B.A., Tewksbury, E., Chapman, G.D., Dorman, D.C., 2010. Pharmacokinetics of radiolabeled tungsten (188 W) in male Sprague-Dawley rats following acute sodium tungstate inhalation. Inhal. Toxicol. 22, 69–76. https://doi.org/10.3109/08958370902913237.

Rajendran, N., Hu, S.-C., Sullivan, D., Muzzio, M., Detrisac, C.J., Venezia, C., 2012. Toxicologic evaluation of tungsten: 28-day inhalation study of tungsten blue oxide in rats. Inhal. Toxicol. 24, 985–994. https://doi.org/10.3109/08958378.2012.745176.

Roedel, E.Q., Cafasso, D.E., Lee, K.W.M., Pierce, L.M., 2012. Pulmonary toxicity after exposure to military-relevant heavy metal tungsten alloy particles. Toxicol. Appl. Pharmacol. 259, 74–86. https://doi.org/10.1016/j.taap.2011.12.008.

Rossi, E.M., Pylkkanen, L., Koivisto, A.J., Nykasenoja, H., Wolff, H., Savolainen, K., Alenius, H., 2010. Inhalation exposure to nanosized and fine TiO2 particles inhibits features of allergic asthma in a murine model. Part. Fibre Toxicol. 7, 35.

Saber, A.T., Bornholdt, J., Dybdahl, M., Sharma, A.K., Loft, S., Vogel, U., Wallin, H., 2005. Tumor necrosis factor is not required for particle-induced genotoxicity and pulmonary inflammation. Arch. Toxicol. 79, 177–182.

Schmid, O., Stoeger, T., 2016. Surface area is the biologically most effective dose metric for acute nanoparticle toxicity in the lung. J. Aerosol Sci. 99, 133–143. https://doi.org/10.1016/j.jaerosci.2015.12.006.

Scholze, M., Silva, E., Kortenkamp, A., 2014. Extending the applicability of the dose addition model to the assessment of chemical mixtures of partial agonists by using a novel toxic unit extrapolation method. PLoS One 9, e88808. https://doi.org/10.1371/journal.pone.0088808.

Schroeder, H.A., Mitchener, M., 1975. Life-term studies in rats: effects of aluminum, barium, beryllium, and tungsten. J. Nutr. 105, 421–427. https://doi.org/10.1093/jn/105.4.421.

Sironval, V., Scagliarini, V., Murugadoss, S., Tomatis, M., Yakoub, Y., Turci, F., Hoet, P., Lison, D., van den Brule, S., 2020. LiCoO2 particles used in Li-ion batteries induce primary mutagenicity in lung cells via their capacity to generate hydroxyl radicals. Part. Fibre Toxicol. 17, 6. https://doi.org/10.1186/s12989-020-0338-9.

Sørli, J.B., Frederiksen, M., Nikolov, N.G., Wedebye, E.B., Hadrup, N., 2022. Identification of substances with a carcinogenic potential in spray-formulated engine/brake cleaners and lubricating products, available in the European Union (EU) - based on IARC and EU-harmonised classifications and QSAR predictions. Toxicology 477, 153261. https://doi.org/10.1016/j.tox.2022.153261.

Sørli, J.B., Jensen, A.C.Ø., Mortensen, A., Szarek, J., Gutierrez, C.A.T., Givelet, L., Loeschner, K., Loizides, C., Hafez, I., Biskos, G., Vogel, U., Hadrup, N., 2023. Pulmonary toxicity of molybdenum disulphide after inhalation in mice. Toxicology 485, 153428. https://doi.org/10.1016/j.tox.2023.153428.

Stoeger, T., Reinhard, C., Takenaka, S., Schroeppel, A., Karg, E., Ritter, B., Heyder, J., Schulz, H., 2006. Instillation of six different ultrafine carbon particles indicates a surface area threshold dose for acute lung inflammation in mice. Environ. Health Perspect. 114, 328–333. https://doi.org/10.1289/ehp.8266.

Stone, V., Miller, M.R., Clift, M.J.D., Elder, A., Mills, N.L., Møller, P., Schins, R.P.F., Vogel, U., Kreyling, W.G., Alstrup Jensen, K., Kuhlbusch, T.A.J., Schwarze, P.E., Hoet, P., Pietroiusti, A., De Vizcaya-Ruiz, A., Baeza-Squiban, A., Teixeira, J.P., Tran, C.L., Cassee, F.R., 2017. Nanomaterials versus ambient ultrafine particles: an opportunity to exchange toxicology knowledge. Environ. Health Perspect. 125, 106002 https://doi.org/10.1289/EHP424.

Tvrda, E., Peer, R., Sikka, S.C., Agarwal, A., 2015. Iron and copper in male reproduction: a double-edged sword. J. Assist. Reprod. Genet. 32, 3–16. https://doi.org/10.1007/s10815-014-0344-7.

Wolff, R.K., Bond, J.A., Henderson, R.F., Harkema, J.R., Mauderly, J.L., 1990. Pulmonary inflammation and DNA adducts in rats inhaling diesel exhaust or carbon black. Inhal. Toxicol. 2, 241–254. https://doi.org/10.3109/08958379009145257.